Analysis of the bromate–ferroin clock reaction

J.H. Merkin [a], A.J. Poole [a,b], S.K. Scott [b], J.D.B. Smith [b] and B.W. Thompson [b]

[a] *Department of Applied Mathematical Studies, University of Leeds, Leeds LS2 9JT, UK*
[b] *School of Chemistry, University of Leeds, Leeds LS2 9JT, UK*

Received 19 June 1995; revised 26 September 1995

The bromate–ferroin clock reaction is studied experimentally and the dependence of the clock or induction time t_{cl} on the initial concentration of various reactants determined. Particular attention is paid to the dependence of t_{cl} on the initial bromide ion concentration $[Br^-]_0$. An analytical theory is also derived based on a subset of the Field–Körös–Noyes mechanism. This analysis reveals several features, including exponential decay of $[Br^-]$ during the induction period followed by a super-exponential decay in the actual clock event, a linear relationship between t_{cl} and $\ln[Br^-]$ over a wide range of $[Br^-]_0$, but departures from this at higher (and lower) concentrations. These features are all confirmed essentially quantitatively by the experimental results. The theory also predicts, and the experiments confirm, that there is a critical bromide ion concentration marking the end of the induction period. This study then provides a firm basis from which to interpret and predict the behaviour of this system in a wider range of experimental situations (such as the reaction-diffusion waves in unstirred media).

1. Introduction

The Belousov–Zhabotinsky (BZ) reaction is probably the most widely-known and studied oscillatory chemical system [1–4]. It comprises the oxidation by an acidified bromate solution of a suitable organic species, catalysed by a single-electron redox reaction typically involving a transition metal ion such as the ferroin-ferriin couple (ferroin = $Fe(II)(phen)_3^{2+}$ where (phen) = 1, 10 phenanthroline). The organic species plays three particular roles in the BZ reaction [5]:

(i) it prevents the accumulation of Br_2, which reacts with the ferroin catalyst to form an insoluble precipitate, either by direct reaction or by reaction with the precursor HOBr to form the brominated organic derivative;
(ii) it reacts with the oxidised form of the catalyst to form the reduced catalyst
(iii) the brominated form also reacts with the oxidised form of the catalyst to produce the reduced form and also to return bromide ion to the system.

Roles (ii) and (iii) are the 'clock resetting' process (generally known as Process C) that allows the reaction to be oscillatory even in thermodynamically closed reactors.

The bromate-ferroin reaction [6] is essentially a subset of the BZ system. An organic species is still included in reactant mixture, but is chosen so that it only plays role (i) above and does not serve to reset the oscillatory clockwork. The behaviour of the bromate-ferroin system is then that of a classic 'clock reaction' with an induction period during which the solution remains in its initial red colour (due to the ferroin) before a relatively sharp colour change to blue as the catalyst is oxidised to the blue ferriin. An example experimental record from a bromide ion specific electrode is shown in fig. 1. This reveals that the bromide ion concentration decreases in an exponential manner (E_{Br} is dependent on $\ln[Br^-]$) over an extended period which is terminated by an super-exponential fall in $[Br^-]$. This change in the evolution corresponds almost exactly to the abrupt colour change seen in the reacting mixture.

The mechanism driving this clock reaction is reasonably well-established [7–9] as the so-called Processes A and B of the BZ mechanism [5]: basically an inhibition stage involving bromide ion and an autocatalytic phase based on the intermediate species $HBrO_2$. The reaction is also of interest as one form of the so-called minimal bromate oscillator (MBO) in well-stirred, flow systems (CSTRs) [10–12]. Early experimental studies of the MBO system employed cerous or manganeous redox catalysts. Subsequent work with the ferroin catalysed system has suggested [13,14] that there are some significant differences arising from the change in redox catalyst [15,16]: a survey of the behaviour of such systems in a CSTR context is given by Gaspar et al. [17]. In this paper we report an analytical study of the bromate-ferroin in the simplified circumstances of a batch system where it gives rise to just a clock reaction. An expression for the dependence of the clock reaction time on the initial concentrations of various species is derived and tested experimentally. Essentially

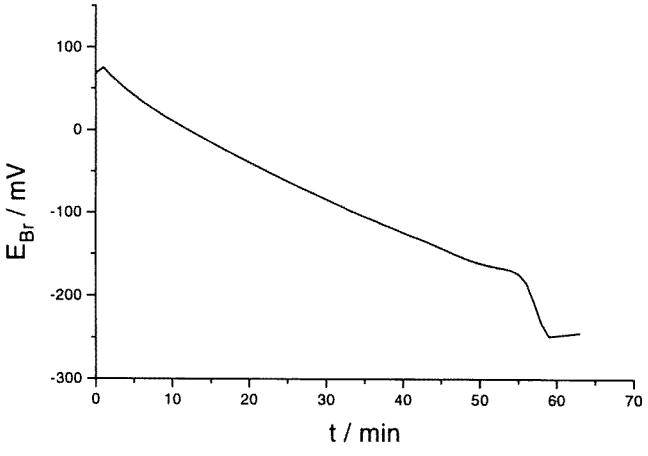

Fig. 1. Variation of potential of bromide ion sensitive electrode (relative to SCE) during bromate-ferroin clock reaction showing exponential dependence of $[Br^-]$ on time before super-exponential decay at end of induction period: initial conditions $[BrO_3^-]_0 = 0.0645$ M, $[H^+]_0 = 0.17$ M, $[Br^-]_0 = 3.2 \times 10^{-3}$ M, $T = 19.8$°C.

quantitative agreement is observed and this allows us to confirm experimentally such important features as the existence and value of the critical bromide ion concentration.

2. Mechanism and governing reaction rate equations

(a) MECHANISM FOR BZ AND BROMATE–FERROIN REACTION

The Field–Körös–Noyes (FKN) mechanism for the BZ reaction consists of three overall 'processes' (the numbering is chosen for consistency with earlier work):

Process A: inhibition by bromide ion

$$\text{(FKN3)}\quad BrO_3^- + Br^- + 2H^+ \rightarrow HBrO_2 + HOBr \qquad \text{rate} = k_3[H^+]^2[BrO_3^-][Br^-]$$

$$\text{(FKN2)}\quad HBrO_2 + Br^- + H^+ \rightarrow 2HOBr \qquad \text{rate} = k_2[H^+][HBrO_2][Br^-]$$

so, overall this has the stoichiometry

$$\text{Process A}\quad BrO_3^- + 2Br^- + 3H^+ \rightarrow 3HOBr$$

Process B: autocatalysis

$$\text{(FKN5)}\quad BrO_3^- + HBrO_2 + H^+ \rightarrow 2BrO_2 + H_2O \qquad \text{rate} = k_5[BrO_3^-][H^+][HBrO_2]$$

$$\text{(FKN6)}\quad BrO_2 + M_{red} + H^+ \rightarrow HBrO_2 + M_{ox} \qquad \text{rate} = k_6[BrO_2][M_{red}][H^+]$$

The radical intermediate species BrO_2 reacts rapidly by step (FKN6) if the catalyst (represented by M_{red}) is ferroin, so these two steps give rise to the overall stoichiometry

$$\text{Process B}\quad BrO_3^- + HBrO_2 + 3H^+ + 2M_{red} \rightarrow 2HBrO_2 + 2M_{ox} + H_2O$$

with (FKN5) being the rate determining step. This autocatalysis in $HBrO_2$ also brings about the oxidation of the redox catalyst. As the $HBrO_2$ concentration increases, the following reaction

$$\text{(FKN4)}\quad 2HBrO_2 \rightarrow BrO_3^- + HOBr + H^+ \qquad \text{rate} = k_4[HBrO_2]^2$$

becomes important in limiting the growth of the autocatalyst.

Process C: resetting

This is a complex process involving both inorganic and organic species. It is believed to involve the bromination (either by HOBr or by Br_2 formed from $HOBr + Br^-$) to form the brominated form of the organic species BrOrg. This then reacts with the oxidised form of the redox catalyst M_{ox}, which may also react with the original organic species. This overall reaction is then represented as

$$\text{Process C} \quad M_{ox} + \{\text{Org} + \text{BrOrg}\} \rightarrow \tfrac{1}{2} f Br^- + M_{red} \quad \text{rate} = k_c[M_{ox}][\text{Org}]$$

where [Org] represents the total concentration of organic species {Org + BrOrg} which will be approximately equal to the initial concentration of the organic reactant. In addition to reducing the redox catalyst, Process C also returns bromide ion to the reaction: the stoichiometric factor f in the above equation is treated as an adjustable parameter and indicates the number of bromide ions produced for every two oxidised catalyst ions reduced.

(b) RATE EQUATIONS FOR BROMATE–FERROIN REACTION

For the bromate-ferroin reaction, Process C does not occur, so we can set $k_c = 0$. This represents a simplification to the kinetics compared with the BZ system but also has some consequences for the choice of nondimensionalisation to be used as the classic Tyson-scalings [18] of the Oregonator model obtained from the FKN scheme above are based on a time scale involving k_c and hence would be inappropriate here.

The reaction rate equations for the species BrO_3^-, $HBrO_2$, Br^- and M_{ox} are thus

$$\frac{dA}{dt'} = -k_3 A H^2 Y - k_5 A H X + k_4 X^2 , \tag{1a}$$

$$\frac{dX}{dt'} = k_3 A H^2 Y - k_2 H^2 X Y + k_5 A H X - 2k_4 X^2 , \tag{1b}$$

$$\frac{dY}{dt'} = -k_3 A H^2 Y - k_2 H X Y , \tag{1c}$$

$$\frac{dZ}{dt'} = 2k_5 A H X , \tag{1d}$$

where $A = [BrO_3^-]$, $X = [HBrO_2]$, $Y = [Br^-]$ and $Z = [M_{ox}]$ are the conventional notation for the BZ system, t' is the time and $H = [H^+]$ which will be assumed to remain constant during the reaction.

The form for eq. (1d) arises as reaction (FKN5) is the rate determining step for Process B in which the oxidation of the redox catalyst occurs, and we will implicitly assume that $[M_{red}]$ is a constant. For later reference we can also note the following values of the rate constants appropriate to 293K: $k_2 = 3 \times 10^6$ M^{-2} s^{-1}, $k_3 = 2$ M^{-3} s^{-1}, $k_4 = 3 \times 10^3$ M^{-1} s^{-1} and $k_5 = 42$ M^{-2} s^{-1}. We also note that the activation energy for step (FKN3) has the value $E_3 = 49.3$ kJ mol^{-1}, allowing this rate constant to be calculated at other temperatures.

3. Dimensionless forms

The following scalings are appropriate for the bromate–ferroin reaction

$$a = A/A_0\,,$$

$$x = X/X_0, \quad X_0 = k_5 A_0 H/2k_4\,,$$

$$y = Y/Y_0, \quad Y_0 = k_5 A_0/k_2\,,$$

$$z = Z/M_{\mathrm{red},0}\,,$$

$$t = t'/t_0, \quad t_0 = 1/k_5 A_0 H\,,$$

together with the dimensionless parameters

$$\delta = 2k_4/k_2 H\,,$$

$$q = 2k_3 k_4/k_2 k_5\,,$$

$$\gamma = k_5 A_0 H/k_4 M_{\mathrm{red},0}\,,$$

$$\sigma = k_5 H/2k_4\,,$$

where A_0 is the initial bromate ion concentration and $M_{\mathrm{red},0}$ is the concentration of the reduced form of the redox catalyst. These yield, from eq. (1),

$$\frac{da}{dt} = -\sigma(qay + ax - \tfrac{1}{2}x^2)\,, \tag{2a}$$

$$\frac{dx}{dt} = x(a - x) - (x - qa)y\,, \tag{2b}$$

$$\delta\frac{dy}{dt} = -(x + qa)y\,, \tag{2c}$$

$$\frac{dz}{dt} = \gamma a x\,. \tag{2d}$$

The scalings for x and y and for the parameter q are the same as those used for the BZ system, but the time scaling here is based on step (FKN5) whilst the parameter δ is the ratio of the parameters ε'/ε that appear in the Tyson scalings. The scaling for the oxidised form of the catalyst is different from that used in the BZ system and is here based on the initial concentration of the reduced catalyst. There are two reasons for this choice: first, if z increases to values close to unity, then the simplification of ignoring the consumption of the reduced catalyst becomes invalid and second, it will be useful to define the end of the clock reaction period in terms of this variable as the experimentalist records this event in terms of the colour change in the reacting mixture. From the rate constants given previously, we have $q = 9.52 \times 10^{-5}$. The parameters δ and σ depend on the initial H^+ concentration (as does γ) but are both typically small compared to unity. The initial conditions are

$$a(0) = 1, \quad x(0) = 0, \quad y(0) = y_0, \quad z(0) = 0, \tag{3}$$

where y_0 is the scaled initial concentration of bromide ion.

4. Initial analysis: reactant consumption neglected, $\sigma = 0$

By assuming that the bromate ions in the system are present in excess we can invoke the pool chemical approximation. This is equivalent to setting σ to zero in eq. (2a), which then gives, from (3),

$$a(t) \equiv 1 \quad \text{for all } t \geqslant 0. \tag{4}$$

Also note that eqs. (2b) and (c) are independent of z and that the solution to eq. (2d) is now dependent only upon x. This leads us to consider the two-dimensional system

$$\frac{dx}{dt} = x(1-x) - (x-q)y, \tag{5a}$$

$$\delta \frac{dy}{dt} = -(x+q)y \tag{5b}$$

in $x \geqslant 0, y \geqslant 0$, still subject to initial conditions (3).

It is readily established that eqs. (5a), (5b) have the stationary states (0, 0) and (1, 0) in the positive quadrant of the (x, y) phase plane and that (0, 0) is a saddle-point and (1, 0) is a stable node for all (positive) values of q and δ. Furthermore, it is straightforward to show that the set

$$= \{(x,y): 0 \leqslant x \leqslant 1, 0 \leqslant y \leqslant y_0\} \tag{6}$$

is an invariant rectangle for the system. Since there can be no closed integral paths within , the Poincaré–Bendixson theorem then guarantees that

$$(x,y) \to (1,0) \quad \text{as } t \to \infty. \tag{7}$$

(a) ASYMPTOTIC ANALYSIS

Here we develop a solution to equations (5a, b) valid for δ small. We also take q to be small and y_0 to be large, formally taking q to be $O(\delta^2)$ and y_0 to be $O(\delta^{-2})$, by writing

$$q = q_0 \delta^2, \quad y_0 = \delta^{-2} v_0, \tag{8}$$

where q_0 and v_0 are both of $O(1)$. These scalings are suggested by their values achieved in the experimental results described below.

A consideration of eqs. (5a), (5b) shows that the solution develops on an initial time scale of $O(\delta^2)$ (region I). This, together with (8), suggests that we write

$$\tau = \delta^{-2}t, \quad x = \delta^2 X, \quad y = \delta^{-2}Y, \tag{9}$$

and expand X and Y as

$$X(\tau;\delta) = X_0(\tau) + \delta X_1(\tau) + \ldots, \quad Y(\tau;\delta) = Y_0(\tau) + \delta Y_1(\tau) + \ldots. \tag{10}$$

At leading order we obtain

$$X_0 = q_0(1 - e^{-v_0\tau}), \quad Y_0 = v_0. \tag{11}$$

The solution can be readily continued to higher order, the details are not important except for the behaviour of the solution as $\tau \to \infty$. We find that

$$X \sim q_0 + \delta^2 q_0/v_0 + \ldots, \quad Y \sim v_0 - 2q_0 v_0 \delta^3 \tau + \ldots \quad \text{as } \tau \to \infty. \tag{12}$$

Thus expansions (10) become non-uniform when τ is $O(\delta^{-3})$, with x and y still $O(\delta^2)$ and $O(\delta^{-2})$, respectively. To continue the solution we move to a second region (region II) where we put $\bar{t} = \delta t$ and again scale x and y by (9). Here the governing equations are to be solved subject to matching to (12). A solution by expanding in powers of δ is suggested, the leading order terms (X_0, Y_0) of which are

$$X_0 = q_0, \quad Y_0 = v_0 e^{-2q_0\bar{t}}. \tag{13}$$

The solution can be continued directly to higher orders and again it is only the behaviour for large $\bar{t}$ that is of interest, we find that

$$x \sim \delta^2\left(q_0 + \delta^2 \frac{q_0}{v_0} e^{2q_0\bar{t}} + \ldots\right), \quad y \sim \frac{1}{\delta^2}\left(v_0 e^{-2q_0\bar{t}} - \frac{\delta^2}{2} + \ldots\right) \quad \text{as } \bar{t} \to \infty. \tag{14}$$

The exponentially growing term in expressions (14) shows that this expansion becomes non-uniform when $\bar{t}$ is $O(\ln(1/\delta^2))$ and so the analysis must be extended to a further region (region III) by a logarithmic shift in $\bar{t}$, given by

$$\bar{t} = \frac{1}{2q_0}\ln\left(\frac{v_0}{\delta^2}\right) + \zeta. \tag{15}$$

Applying (15) in (14) shows that, in region III, x is still of $O(\delta^2)$ though y is now of $O(1)$. Thus in region III we still put $x = \delta^2 X$ but leave y unscaled. This leads to the equations, at leading order,

$$X = (X - q_0)y, \quad \frac{dy}{d\zeta} = -(X + q_0)y, \tag{16}$$

to be solved subject to the matching conditions

$$X \sim q_0(1 + e^{2q_0\zeta} + \ldots), \quad y \sim e^{2q_0\zeta} - \tfrac{1}{2} + \ldots \quad \text{as } \zeta \to -\infty. \tag{17}$$

The first of these equations gives $X = q_0 y/(y - 1)$ and hence

$$\frac{dy}{d\zeta} = -\frac{q_0(2y-1)y}{y-1}. \tag{18}$$

The solution which satisfies the conditions as $\zeta \to -\infty$ is then obtained as

$$y = \tfrac{1}{2}e^{-2q_0\zeta}(1+\sqrt{1-2e^{2q_0\zeta}}), \quad X = \frac{q_0}{\sqrt{1-2e^{2q_0\zeta}}}. \tag{19}$$

These expressions become singular ($X \to \infty, y \to 1$) at $\zeta = \zeta_0 = \frac{1}{2q_0}\ln(\frac{1}{2})$, with

$$X \sim \sqrt{\frac{q_0}{2}}(\zeta_0-\zeta)^{-1/2} + \ldots, \quad y \sim 1 + \sqrt{2q_0}(\zeta_0-\zeta)^{1/2} \quad \text{as } \zeta \to \zeta_0^-. \tag{20}$$

In order to remove the singularity at ζ_0 we require a further region (region IV) in which we put

$$X = \delta^{-1/3}\bar{X}, \quad y = 1+\delta^{2/3}\bar{y}, \quad \zeta = \zeta_0 + \delta^{2/3}\eta. \tag{21}$$

The leading order problem then becomes

$$\frac{d\bar{X}}{d\eta} = q_0 - \bar{X}\bar{y}, \quad \frac{d\bar{y}}{d\eta} = -\bar{X}, \tag{22}$$

subject to, from (20),

$$\bar{X} = \sqrt{\frac{q_0}{2}}(-\eta)^{1/2} + \ldots, \quad \bar{y} \sim \sqrt{2q_0}(-\eta)^{1/2} + \ldots \quad \text{as } \eta \to -\infty. \tag{23}$$

Differentiating the second equation in (22) once with respect to η, and eliminating $\bar{X}$ using the first equation, we obtain a second order equation for $\bar{y}$ which can then be integrated once to give, on satisfying the matching conditions,

$$\frac{d\bar{y}}{d\eta} + \tfrac{1}{2}\bar{y}^2 + q_0\eta = 0. \tag{24}$$

The solution to eq. (24), subject to (23), can be expressed in terms of Airy functions as

$$\bar{y} = \frac{-2A_i'\left[-\left(\frac{q_0}{2}\right)^{1/3}\eta\right]}{A_i\left[-\left(\frac{q_0}{2}\right)^{1/3}\eta\right]}. \tag{25}$$

From this expression we can see that the solution becomes singular at

$$\eta = \eta_0 = -\left(\frac{2}{q_0}\right)^{1/3} s_0, \tag{26}$$

where $s_0 = -2.338107$ is the first zero of $A_i(s)$, with

$$\bar{X} \sim \frac{2}{(\eta_0-\eta)^2}, \quad \bar{y} \sim \frac{-2}{\eta_0-\eta} \quad \text{as } \eta \to \eta_0^-. \tag{27}$$

We now require a further region (region V) in order to remove the singularity at η_0, in which we put $\eta = \eta_0 + \delta^{1/3}\xi$, $X = \delta^{-1}\hat{X}$ and leave y unscaled. This gives the leading order problem for region V as

$$\frac{d\hat{X}}{d\xi} = \hat{X} - \hat{X}y, \quad \frac{dy}{d\xi} = -\hat{X}y, \tag{28}$$

with, from (27),

$$\hat{X} \sim \frac{2}{(-\xi)^2} + \ldots, \quad y \sim 1 - \frac{2}{(-\xi)} + \ldots \quad \text{as } \xi \to -\infty. \tag{29}$$

Equations (28) can be combined to give, on satisfying (29),

$$\hat{X} = y - \log(y) - 1. \tag{30}$$

It is not possible to obtain closed-form expressions for $\hat{X}$ and y in terms of ξ, though we note that $y \sim e^{-\hat{X}}$ as $\hat{X} \to \infty$. Further consideration of eqs. (28) then shows that $\hat{X}$ is exponentially large for ξ large, with

$$\hat{X} \sim A_0 e^{\xi}, \quad y \sim \exp(-A_0 e^{\xi}) \quad \text{as } \xi \to \infty \tag{31}$$

for some positive constant A_0, which is independent of the parameters of the system but which cannot be determined explicitly.

To complete the solution, we need a final region (region VI) where $y \equiv 0$, x is $O(1)$, and, from (31), we require a further logarithmic shift in the time variable,

$$\xi = \ln\left(\frac{1}{\delta}\right) + \bar{\xi}. \tag{32}$$

The governing equations in this region reduce to

$$\frac{dx}{d\bar{\xi}} = x(1-x), \quad x \sim A_0 e^{\bar{\xi}} + \ldots \quad \text{as } \bar{\xi} \to -\infty. \tag{33}$$

On solving (33) we obtain

$$x = \frac{A_0 e^{\bar{\xi}}}{1 + A_0 e^{\bar{\xi}}} \tag{34}$$

from which it follows that $x \to 1$ as $\bar{\xi} \to \infty$. This completes the development of the solution for $\delta \ll 1$.

(b) NUMERICAL RESULTS

Equations (5a), (5b) were solved numerically using a standard NAG routine (D02EBF). Care had to be taken to use a sufficiently small time step so that the initial development of the solution on the $O(\delta^2)$ time-scale in region I was represented accurately. Results for $\delta = 1.17 \times 10^{-2}$, $q = 9.52 \times 10^{-5}$, $y_0 = 4500$ are

plotted in fig. 2(a). These results show, as predicted by the asymptotic analysis for δ small, that y falls monotonically while x remains small, with $x \approx q$ over most of this range (region II). (The initial behaviour of the solution (region I) is difficult to observe in this figure). After a further time has elapsed x starts to increase, slowly at first (region IV and V), followed by a very rapid rise in its value (region VI) before its final value is attained. The very rapid fall in y associated with the singularities in regions III and IV resulting in the super-exponential decay in region V (expression (31)) is difficult to see in fig. 2(a), though it can be observed on a much closer examination of the numerical results and is shown in fig. 2(b). It is interesting to note that this super-exponential decay is clearly observed in the experimental results, fig. 1, which gives a strong confirmation of our theory.

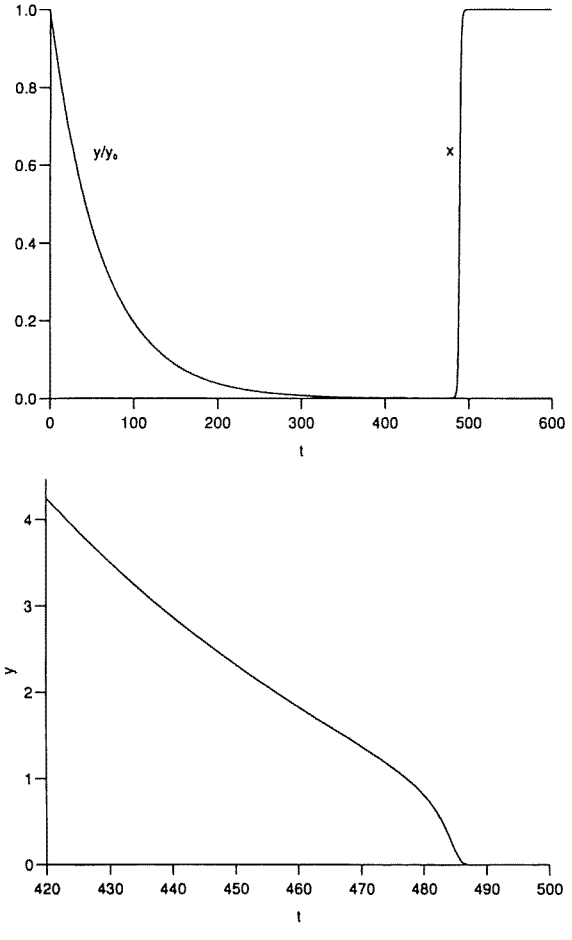

Fig. 2. Computer dependence of dimensionless $[Br^-]$ and $[HBrO_2]$ (y and x, respectively) on (dimensionless) time showing exponential decay of y during a period in which $x \approx q$, followed by autocatalytic growth of x: $q = 9.52 \times 10^{-5}$, $\delta = 0.0117$, $y_0 = 4500$, $\sigma = 0$ (bromate consumption ignored). Note sharpness of 'clock' process in autocatalytic phase.

(c) INDUCTION TIME OF THE CLOCK REACTION

Although the induction time of a clock reaction is observed to occur when there is a rapid colour change, it is difficult to define exactly when this occurs in terms of the variables x, y and z. Here the clock reaction is determined by the oxidation of the catalyst and the associated colour change from red to blue, which in the original system (2a)–(2d) is represented by z reaching a specific value. However, since z is related to x by eq. (2d), we can alternatively define the induction time t_{cl} as the time at which x reaches a specific value, x_{cl}, (say), where we require x_{cl} to be significantly greater than q. Since x reaches x_{cl} in region VI, where x is increasing exponentially rapidly (see fig. 2), the induction time will be insensitive to the value of x_{cl} chosen. For the majority of the induction time, x remains small and starts to rise in value only at the end of region III. From (15) we then have that the (dimensionless) induction time occurs when $\zeta = \zeta_0$ (with $y \to 1$), giving

$$t_{cl} = \frac{1}{2q_0}\ln\left(\frac{v_0}{2\delta^2}\right) = \frac{\delta}{2q}\ln\left(\frac{y_0}{2}\right) \tag{35}$$

to leading order. Expression (35) shows that t_{cl} is $O(\ln(y_0/2))$ and to demonstrate this we integrated eqs. (5a), (5b) numerically for a range of values of y_0 (with δ and q as above) taking $x_{cl} = 0.5$. The results are shown in fig. 3, where we plot t_{cl} against $\log_{10}(y_0)$. This figure shows that the agreement between the theoretical (expression (35)) and numerically computed values is extremely good, with the results lying on a straight line over many orders of magnitude in y_0; the divergence from this straight line form is seen only when y_0 is $O(1)$ when the theory developed above is not applicable. Moreover, this straight line has a slope of 141, also in agreement with (35) and, if continued, would cross the $t_{cl} = 0$ axis at $y_0 = 2$, again in agreement with (35).

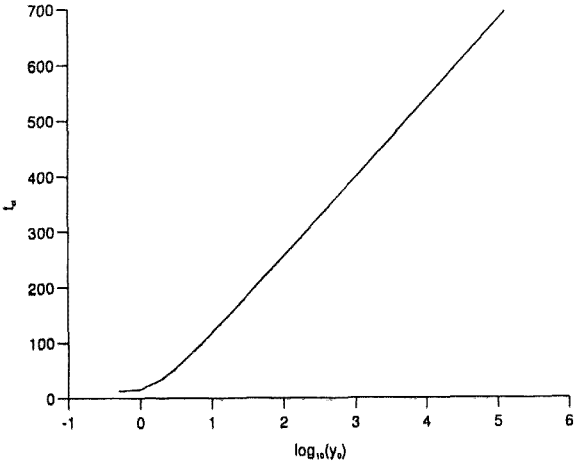

Fig. 3. Numerically computed clock times for a system without bromate consumption ($\sigma = 0$) showing linear dependence of t_{cl} on $\log(y_0)$ for y_0 sufficiently large.

Finally, we note that the dimensional induction time t_{cl} is given from (35) by

$$t'_{cl} = \frac{1}{2k_3[BrO_3^-]_0[H^+]^2} \ln\left(\frac{k_2[Br^-]_0}{2k_5[BrO_3^-]_0}\right). \tag{36}$$

5. Experimental

Stock solutions of the following reactants were prepared separately and without further purification: $KBrO_3$ (AR grade, Fisons), NaBr (SLR grade, Fisons), H_2SO_4, 4-cyclohexene-1,2-dicarboxylic acid (obtained as cis-1,2,3,6-tetrahydrophthalic anhydride, Aldrich 98%), ferroin from iron(II) sulphate (AR grade) and 1,10 phenanthroline hydrate (Sigma: 1 : 3 molar proportions). Appropriate quantities were mixed to obtain the desired initial concentrations, with H^+ being added last and the time zero being taken at the point of half-addition of the acid. The clock time was determined by visual estimate of the change of the solution colour from red to blue. Preliminary experiments establish the inverse first-order dependence on the initial bromate ion concentration and also the independence of t_{cl} on the ferroin and 4-cyclohexene-1,2-dicarboxylic acid concentrations. Here we concentrate on the dependence of t_{cl} on $[H^+]_0$ and on $[Br^-]_0$.

(a) DEPENDENCE ON INITIAL ACID CONCENTRATION

The clock times were measured for an initial mixture of composition $[BrO_3^-]_0 = 0.0645$ M, [4-cyclohexene-1,2-dicarboxylic acid]$_0 = 0.0645$ M, $[Br^-]_0 = 0.0323$ M and [ferroin]$_0 = 8.1 \times 10^{-4}$ M with $[H_2SO_4]_0$ varied between 0.111 M and 0.233 M, giving clock times between 550 and 2800 s at 291 K. The variation of t_{cl} with $[H_2SO_4]_0$ is recorded in table 1. Also shown in the table is the corresponding initial H^+ concentration. For the relatively high acid concentrations used in this study we cannot assume complete dissociation of H_2SO_4; $[H^+]_0$ has been estimated by making a linear fit to the data quoted by Robertson and Dunford [19]. Over the range $0.1 < [H_2SO_4]_0/M < 0.5$ this is given by

Table 1
Variation of clock time with $[H^+]_0$.

$[H_2SO_4]_0$/M	$[H^+]_{0,calc}$/M	$(t_{cl} \pm 10)$/s
0.111	0.147	2760
0.129	0.170	1740
0.155	0.204	1127
0.181	0.237	1004
0.207	0.270	810
0.233	0.303	558

$$[H^+]/M = 0.006 + 1.276[H_2SO_4]/M \tag{37}$$

with a regression coefficient of 0.99999.

The predicted dependence of t_{cl} on $[H^+]_0$ is tested by determining the slope n of the $\log[H^+]$-$\log(t_{cl})$ plot, figure 4(a). The data in table 1 give $n = -2.01 \pm 0.18$, indicating good agreement with the predicted value $n = -2$. A plot of t_{cl} versus $1/[H^+]^2$, fig. 4(b), gives a straight line of gradient $m = 58 \pm 5$ M^2 s (or $m = 54.3 \pm 1.3$ if the line is constrained to pass through the origin). According to eq. (36), the slope of this plot should be given by

$$m = \frac{1}{2k_3[BrO_3^-]_0} \ln\left(\frac{k_2[Br^-]_0}{2k_5[BrO_3^-]_0}\right). \tag{38}$$

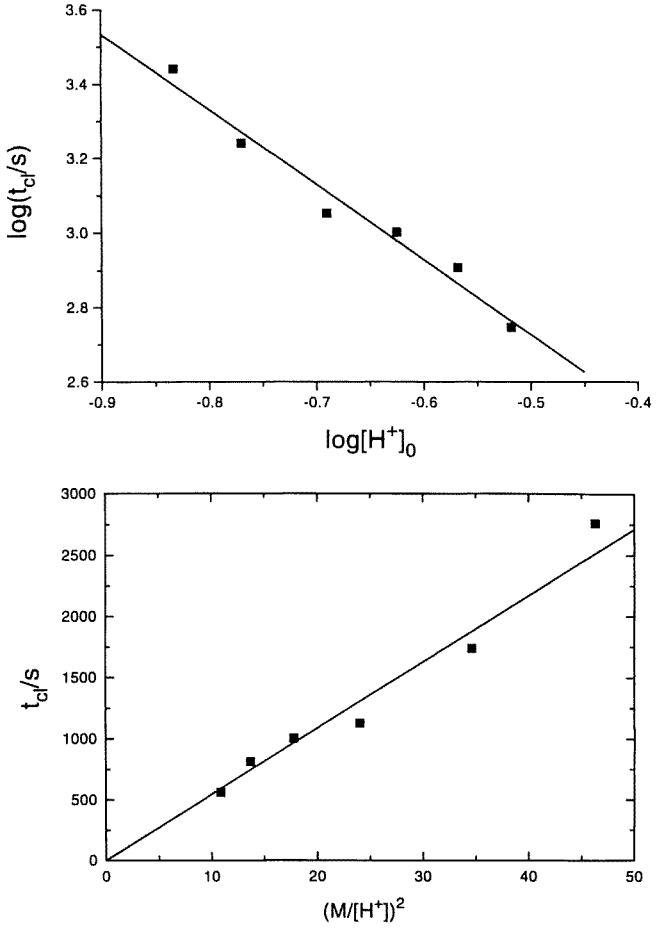

Fig. 4. (a) log–log plot of induction period versus $[H^+]$ indicating inverse square dependence (slope $= -2.01 \pm 0.18$); (b) inverse square plot of t_{cl} versus $1/[H^+]^2$.

Substituting the appropriate values for the initial concentrations and the reaction rate constant k_3 at 291 K into eq. (38) then, we obtain the predicted value of m,

$$m_{\text{calc}} = 46.7 \text{ M}^2 \text{ s}, \tag{39}$$

indicating essentially quantitative agreement within the experimental precision.

We may also note that the slope of the linear portion in fig. 1 (the plot of E_{Br} versus t) should, according to the analysis of the previous section, be given by

$$\text{slope} = \frac{dE_{\text{Br}}}{dt} = -\frac{RT}{nF} \times 2k_2[\text{BrO}_3^-][\text{H}^+]^2 . \tag{40}$$

Taking the initial H^+ concentration as calculated from eq. (37) above, we thus predict for the conditions in the figure a slope of -11.3 mV min^{-1} which again compares favourably with the experimental value of -11.9 mV min^{-1}.

(b) DEPENDENCE ON INITIAL BROMIDE ION CONCENTRATION

A series of experiments with the same $[\text{BrO}_3^-]_0$, [4-cyclohexene-1,2-dicarboxylic acid]$_0$ and [ferroin]$_0$ as above and with $[\text{H}_2\text{SO}_4]_0 = 0.129$ M in which 6×10^{-5} M $< [\text{Br}^-]_0 < 0.0323$ M, were performed at 298 K giving clock times in the range 250 s $< t_{\text{cl}} <$ 2250 s. The lower end of this range still corresponds to a bromide ion concentration an order of magnitude greater than that arising from impurities in the bromate stock (which we may estimate from the manufacturer's specifications to be less than 6×10^{-6} M). The maximum initial bromide ion concentration is determined by the condition [4-cyclohexene-1,2-dicarboxylic acid]$_0 > 1.5[\text{Br}^-]_0$ which must be satisfied in order to prevent the formation of molecular Br_2.

The variation of t_{cl} with $\log[\text{Br}^-]_0$ is shown in fig. 5 along with the predicted

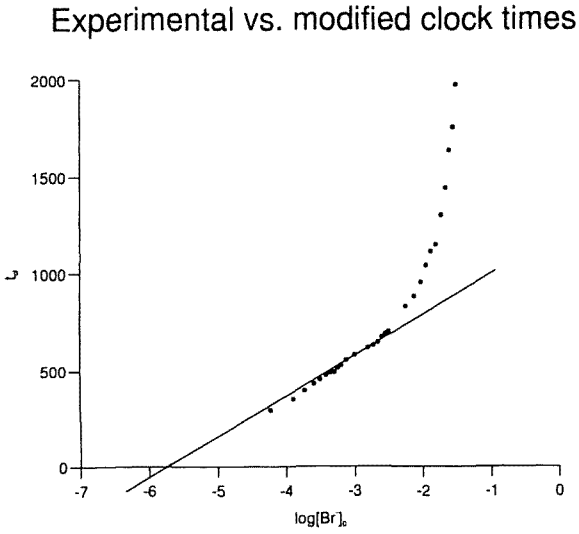

Fig. 5. Comparison of analytical prediction (eq. (36)) with experimental dependence (shown as points) of clock times on $\log[\text{Br}^-]$ (model with bromate consumption ignored, $\sigma = 0$).

clock time on the basis of eq. (36). First, we note that over the range $-4.2 < \log[Br^-]_0 < -2.4$, (equivalent to $[Br^-]_0$ in the range 4.0×10^{-3} to 6.3×10^{-5} M) the behaviour is approximately linear as predicted by our theory. The slope of a regression line for the data over this range has the value $m = 244(\pm 30)$ s, which compares with the predicted slope $2.303/2k_3[BrO_3^-]_0[H^+]_0^2 = 220$ s (taking $[H^+]_0 = 0.17$ M and $k_3 = 2.81$ M^{-3} s^{-1} appropriate to 298 K). The agreement is again well within the experimental accuracy.

Also of interest, is the departure from the logarithmic dependence of t_{cl} on $[Br^-]_0$ at high initial bromide ion concentrations. To account for this change in behaviour, we must return to our analysis and recognise that if $[Br^-]_0/[BrO_3^-]_0$ is not small, then significant amounts of the reactant bromate ion will be consumed by the end of the induction period. This may then invalidate our assumption $[BrO_3^-] \approx [BrO_3^-]_0$, i.e. $a \equiv 1$ in the analysis of section 4.

6. Effects of bromate consumption

The experimental results presented in fig. 5 show that for high initial bromide ion concentrations, the simple logarithmic dependence of the induction time as given by eq. (36) is no longer valid, with t_{cl} appearing to tend towards some asymptotic limit. The reason for this divergence between experiment and theory becomes apparent if we consider the stoichiometry of Process A (section 2) which indicates that one bromate ion is consumed for every two bromide ions that react. In the region of high initial bromide ion concentration, the concentration of the bromate ions may no longer be considered to be in excess and the assumptions of the pool chemical approximation for this reactant are no longer valid. Thus at high $[Br^-]_0$, we must consider the system (2a)–(2d) with reactant consumption included.

This can be done following closely the analysis in section 4(a), again on the basis of δ being small and y_0 and q scaled via eq. (8). In the present context, the parameter σ is now non-zero though small: formally we set $\sigma = \sigma_0\delta$, where σ_0 is $O(1)$. The solution then develops over the different time regions as before, with the clock induction time being given, to leading order, as the time at which the singularity develops in region III (this can be smoothed out, as before, through regions IV and V). The details of the analysis are not particularly important or particularly different from the previous case. The resulting expression for the dimensionless clock induction time is

$$t_{cl} = \frac{1}{\delta q_0(2 - \sigma_0 v_0)} \ln\left(\frac{v_0}{2\delta^2}\right). \tag{40}$$

This equation reduces to that previously derived form, eq. (35), in the limit $\sigma = 0$.

Expression (40) requires

$$y_0\sigma\delta < 2, \quad \text{i.e.} \quad [Br^-]_0 < 2[BrO_3^-]_0. \tag{41}$$

This inequality is expected from the stoichiometry and expresses the fact that sufficient initial bromate is required so that all the bromide can be removed through Process A. If the inequality is not satisfied, our analysis shows, as expected, that $[Br^-]$ cannot fall sufficiently to trigger the clock via Process B and $[HBrO_2]$ remains small throughout.

The predicted dependence of the (dimensional) induction time on initial bromide ion concentration given by eq. (40) for the case $\sigma = 1.197 \times 10^{-3}$ is compared with the experimental results of section 5 in fig. 6 where the effect of bromate consumption at high $[Br^-]_0$ is apparent. Induction periods have also been computed numerically by direct integration of the full set of eqs. (2a)–(2d), allowing for bromate consumption. For these parameter value, the results are indistinguishable from the analytical predictions. This test serves to suggest that consumption of bromate is the cause of the departure of t_{cl} from its simple linear dependence on $\ln[Br^-]_0$ rather than other minor effects such as the reversibility of step (FKN3): even small amounts of bromate consumption (of the order of a few percent) serve to lengthen t_{cl} by altering the pseudo-first order character of the kinetics in Process A.

7. Discussion and conclusions

The bromate clock reaction is something of a standard reaction kinetics experiment in which the influence of initial bromate and H^+ ion concentrations on the

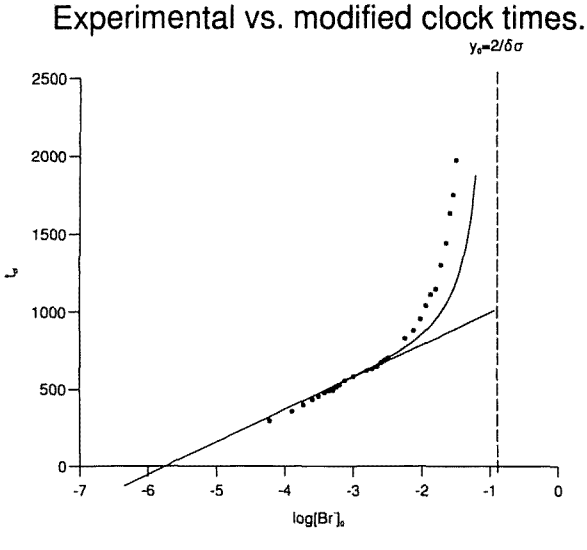

Fig. 6. Comparison of analytical predictions of clock time (eq. (40)) with bromate consumption included with simple analytical prediction (no bromate consumption) and experimental results (shown as points).

clock time are frequently investigated. The present paper has considered a variation on that system and, in particular, has concentrated on the more subtle dependence of t_{cl} on the initial bromide ion concentration. The results presented above show that the basic inorganic subset of reactions in the FKN model provide a basis for at least a semi-quantitative representation of the actual behaviour in the bromate-ferroin system. We have also confirmed the independence of t_{cl} on the initial ferroin concentration. The ability to model this reaction in detail is to become important in work to be reported later in which the reaction-diffusion wave phenomena associated with this reaction in unstirred systems (and, in particular, in situations where the ferroin catalyst is immobilised on a membrane support) are examined. In such situations, any such waves will propagate against the slow change in the unreacted solution ahead as the clock reaction proceeds. We can also anticipate that ease of initiation of a wave will be influenced the concentration of Br^- locally at the initiation site and, hence, on the time elapsed between the mixing of the solutions and the application of the initiation stimulus. Such features will be presented in a later paper.

For now, we may note that our analysis has successfully predicted (i) the basic, exponential decrease of $[Br^-]$ during the induction period as indicated by the linear plot of E_{Br} versus time – a very similar decay of $[Br^-]$ occurs in the BZ reaction during its Process A phase and which plays the major role in determining the period between the oscillatory oxidation events in that system; (ii) a super-exponential change at the end of the induction period – again, such a feature arises in the full BZ system although then there is a subsequent bromide ion production stage; (iii) the existence of a *critical bromide ion concentration*, given by $[Br^-]_{cr} = k_5[BrO_3^-]/k_2$ – this is an important concept in the full BZ system and hence the present work provides quantitative confirmation that this marks the transition from Process A to Process B in that reaction too; (iv) a linear dependence of t_{cl} on $\ln[Br^-]$ provided $[Br^-]_0 \ll [BrO_3^-]_0$; (v) a departure from such a linear dependence at high $[Br^-]_0$, with t_{cl} lengthening under the influence of bromate ion consumption; (vi) an upper limit on $[Br^-]_0$, above which clock behaviour is not observed; (vii) a departure from the linear dependence of t_{cl} on $\ln[Br^-]$ at very low $[Br^-]_0$. The latter is a feature only of the numerical and experimental results: our analytical theory has not been developed for the lowest initial bromide ion concentrations and, subsequently, predicts that t_{cl} becomes negative at very low $[Br^-]_0$: such concentration are, however, unimportant in practice as they relate to values lower than the impurity levels in the bromate stock.

We may note that the 'reactant consumption included' theory ($\sigma \neq 0$) predicts a dependence of t_{cl} on $\ln[Br^-]$ of the correct functional form, but that the experimental clock induction time approaches an asymptotic limit faster than the analytical result. This is probably due to other factors, such as net accumulation of bromine and hence precipitation of the redox catalyst for systems high bromide concentrations and, possibly, due to the reversibility of step (FKN3). Also if the concentration of $HBrO_2$ becomes large, then a significant proportion of the

reduced catalyst may be oxidised in Process B. This would render invalid our assumption that the concentration of ferroin can be treated as a constant: in that event, reaction (FKN5) may no longer be rate determining in this process. However, as shown above, the induction period is primarily determined by the time taken for Process A to reduce $[Br^-]$ to the critical bromide ion concentration, and thus small changes to Process B are not expected to influence t_{cl} significantly. In a similar way, we would also expect to find only minor changes by replacing the ferroin/ferriin couple by the cerous/ceric ion or other redox catalysts for which the kinetics of Process B are subtly different.

References

[1] B.P. Belousov, Ref. Rad. Med. 145 (1959) 145.
[2] A. Zhabotinsky, Dokl. Akad. Nauk. SSSR 157 (1964) 392.
[3] R.J. Field and M. Burger (eds.), *Oscillations and Traveling Waves in Chemical Systems* (Wiley, New York, 1985).
[4] S.K. Scott, *Oscillations, Waves and Chaos in Chemical Kinetics* (Oxford University Press, 1994).
[5] R.J. Field, E. Koros and R.M. Noyes, J. Am. Chem. Soc. 94 (1972) 8649.
[6] K. Showalter, J. Phys. Chem. 85 (1981) 440.
[7] K. Bar-Eli and R.M. Noyes, J. Phys. Chem. 82 (1978) 1352.
[8] R.J. Field, J. Chem. Phys. 63 (1975).
[9] K. Showalter, R.M. Noyes and K. Bar-Eli, J. Chem. Phys. 60 (1978) 2514.
[10] W. Geiseler, Ber Bunsenges. Phys. Chem. 86 (1982) 721; J. Phys. Chem. 86 (1982) 4394.
[11] M. Orban, P. De Kepper and I.R. Epstein, J. Am. Chem. Soc. 104 (1982) 2657.
[12] W. Geiseler and K. Bar-Eli, J. Phys. Chem. 85 (1981) 908.
[13] E. Koros, M. Burger and A. Kis, React. Kinet. Catal. Lett. 1 (1974) 475.
[14] A.B. Rovinsky and A.M. Zhabotinsky, React. Kinet. Catal. Lett. 11 (1979) 205.
[15] A.B. Rovinsky and A.M. Zhabotinsky, J. Phys. Chem. 88 (1984) 6081.
[16] R.M. Noyes, J. Am. Chem. Soc. 102 (1980) 4644.
[17] V. Gaspar, G. Basza and M.T. Beck, J. Phys. Chem. 89 (1985) 5495.
[18] J.J. Tyson, J. Phys. Chem. 86 (1982) 3006.
[19] E.B. Robertson and H.B. Dunford, J. Am. Chem. Soc. 86 (1964) 5080.